Earth and Planetary Science Letters 272 (2008) 531–540

Contents lists available at ScienceDirect

Earth and Planetary Science Letters

journal homepage: www.elsevier.com/locate/epsl

Slow exhumation of UHP terranes: Titanite and rutile ages of the Western Gneiss Region, Norway

A.R.C. Kylander-Clark *, B.R. Hacker, J.M. Mattinson

University of California, Santa Barbara, CA, 93106-9630, USA

ARTICLE INFO

Article history:
Received 20 February 2008
Received in revised form 14 May 2008
Accepted 14 May 2008
Available online 28 May 2008

Editor: R.W. Carlson

Keywords:
titanite
rutile
geochronology
ultrahigh-pressure
Norway

ABSTRACT

U–Pb ages of titanite and rutile were obtained from the central Western Gneiss Region, Norway, to assess the style and timing of exhumation and cooling of the Western Gneiss UHP terrane. Approximately half of the titanite ages are concordant, the majority of which yield a limited age range from 393 to 390 Ma. The other titanite data are discordant, and define discordia arrays with upper intercept ages of either ~938 Ma or ~1.6 Ga, and a lower intercept of ~389 Ma. Concordant rutile analyses range from 385 to 392 Ma. Both titanite *and* rutile ages young WNW toward the core of the orogen and are ~4 Ma older than $^{40}Ar/^{39}Ar$ muscovite ages, corresponding to a cooling rate of ~90 °C/Ma. A well-defined boundary between concordant and discordant titanite ages, in combination with the WNW-increasing *P–T* gradient and the similarity between muscovite cooling ages in the east and eclogite ages in the west, suggests that the WGR remained coherent throughout its exhumation history, and was progressively unroofed from east to west. A 390.2 ± 0.8 Ma titanite in the Sørøyane UHP domain indicates that exhumation occurred at a vertical rate of ~7 mm/yr for ~12 Ma. These rates are slower than estimates from smaller UHP terranes, but similar to other large UHP terranes, suggesting that there may be fundamental differences in the mechanisms controlling the evolution of large UHP terranes that undergo protracted subduction and exhumation, and smaller UHP terranes that undergo rapid subduction and exhumation.

1. Introduction

The Western Gneiss Region (WGR) of western Norway has long been a primary location for the study of geodynamic processes associated with ultrahigh-pressure (UHP) tectonics as it contains one of the largest (>60,000 km^2) and best-exposed HP terranes on the planet. Much of our understanding of some of the world's most enigmatic processes has been deduced from the inferred history of the WGR, but a large part of its history remains unresolved.

The WGR is composed of crystalline basement of primarily granodioritic to tonalitic composition (the Western Gneiss Complex, WGC), and a series of overlying allochthons emplaced during the initial stages of the Caledonian orogeny (~435–400 Ma, Roberts and Gee, 1985; Hacker and Gans, 2005). Peak pressures and temperatures increase westward, reflecting down-to-the-west subduction of the western edge of the Baltica craton (WGC) beneath Laurentia during the late stages of orogenesis (e.g., Griffin et al., 1985). The western portion of the WGR contains three distinct UHP regions (Fig. 1, Root et al., 2005), the northernmost of which records peak pressures >3.4 GPa (Dobrzhinetskaya et al., 1995; van Roermund and Drury, 1998; Terry et al., 2000b; van Roermund et al., 2001; Carswell et al., 2006). Peak temperatures are ~700–800 °C across the three UHP regions, but decrease south of Nordfjord to ~600–650 °C (Fig. 1, Cuthbert et al., 2000; Labrousse et al., 2004; Walsh and Hacker, 2004; Hacker and Gans, 2005; Carswell et al., 2006; Hacker, 2006; Young et al., 2007). The post-(U)HP exhumation of the WGR was nearly isothermal, with metamorphic minerals recording passage through amphibolite-facies conditions down to pressures as low as 0.6 GPa at 750 °C (Fig. 2, summary in Hacker, 2007).

Exhumation of the WGR imprinted a pervasive, westward-increasing E–W horizontal stretch during decompression-related retrograde amphibolite-facies metamorphism (e.g., Andersen, 1998) and caused local *in situ* melting (Labrousse et al., 2002). Such intrusive bodies form important time and strain markers for studying the exhumation process, but they are similar in appearance and difficult to distinguish from older Phanerozoic and Proterozoic intrusions (Lundmark and Corfu, 2007). Determining the ages of intrusive bodies across the WGR is therefore important to constraining the exhumation mechanism.

Several of the best-studied UHP terranes worldwide are known to have undergone rapid exhumation. The exhumation rate of the WGR is known in general terms (e.g., Root et al., 2005; Hacker, 2007), but it is constrained mostly by peak metamorphic ages locked in at mantle depths and by $^{40}Ar/^{39}Ar$ cooling ages frozen in at mid-crustal levels. The history of the intervening 300 °C of cooling is poorly known, and this

* Corresponding author. Tel.: +1 805 893 7999; fax: +1 805 893 2314.
E-mail address: akylander@umail.ucsb.edu (A.R.C. Kylander-Clark).

0012-821X/$ – see front matter © 2008 Elsevier B.V. All rights reserved.
doi:10.1016/j.epsl.2008.05.019

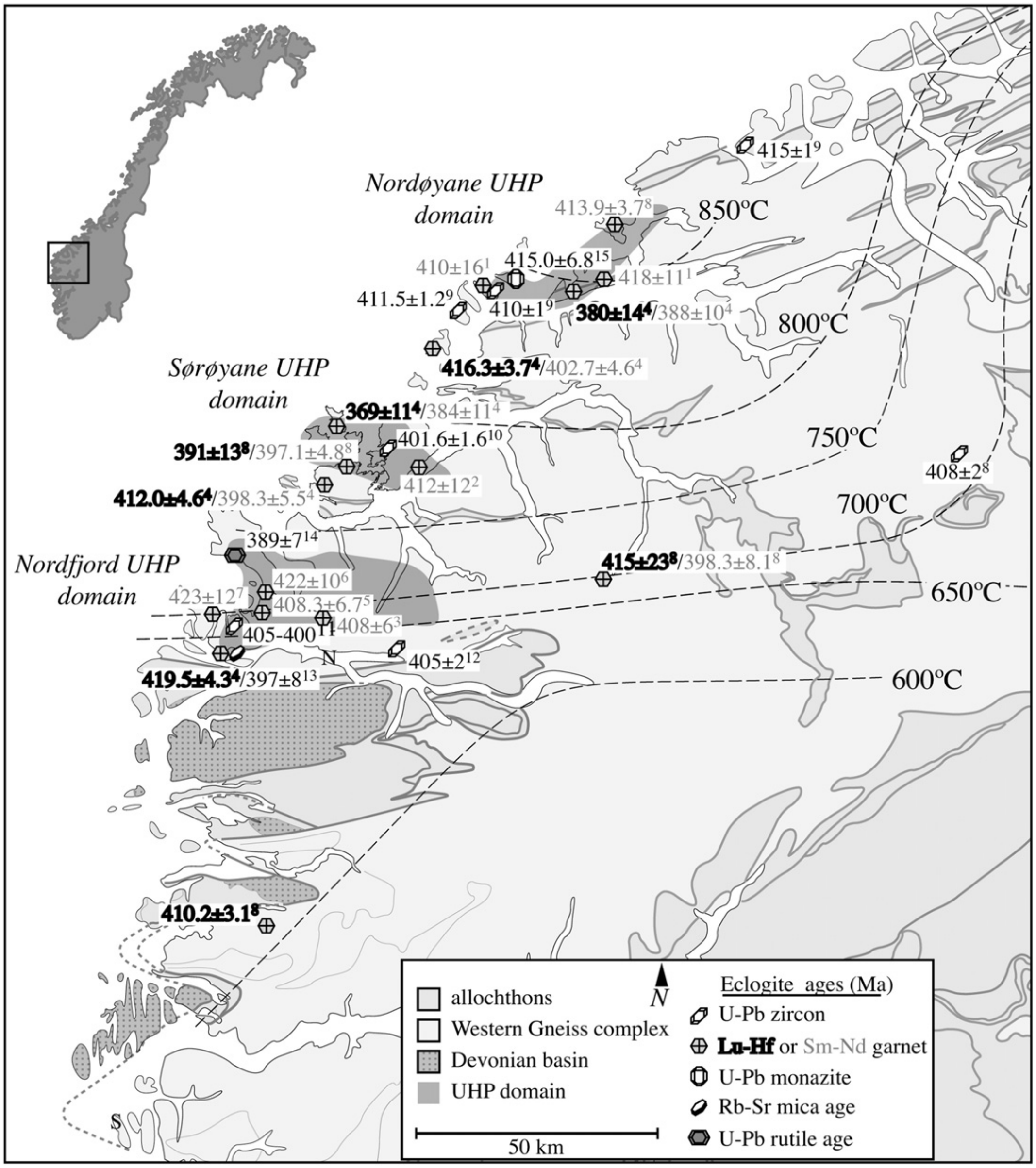

Fig. 1. Western Gneiss Region, western Norway, showing approximate peak temperatures and the following eclogite ages: 1) Mørk and Mearns (1986), 2) Jamtveit et al. (1991), 3) Mearns (1986), 4) Kylander-Clark et al. (2007b), 5) Carswell et al. (2003a), 6) Brueckner (personal comm.), 7) Griffin and Brueckner (1980), 8) Kylander-Clark et al. (2007a), 9) Krogh et al. (2004), 10) Carswell et al. (2003b), 11) Root et al. (2004), 12) Young (2007), 13) Griffin and Brueckner (1985), 14) Schärer and Labrousse (2003), 15) Terry et al. (2000). S = sample location for titanite not shown in Fig. 3; N = Nordfjord.

limits our ability to understand the exhumation mechanism. Understanding the exhumation mechanism requires comprehensive measurements of the cooling rate and its spatial variation throughout the WGR.

Continent-subduction models make predictions of the style and rate at which tectonic processes occur. In particular, the timing and magnitude of melting, and the rates of exhumation and cooling—and their temporal and spatial variation—can be used to distinguish among tectonic models for the formation and exhumation of UHP terranes. These models are best tested through field observations, and can be improved with more accurate input parameters. For the case of Norway, defining how exhumation, melting, and cooling varied spatially from the core of the orogen to the hinterland allows one to discriminate among several models that predict different aspects of the retrograde evolution of the region: 1) Was the WGR exhumed as one coherent body, a few large bodies, or was it well mixed/disrupted (e.g., Wain, 1997; Wain et al., 2000)? 2) Did the WGR stall and flatten at the Moho (Walsh and Hacker, 2004) or was it progressively exhumed at constant rates? 3) Did the slab rise as a diapir through the mantle or was it extruded as a slab (Hacker, 2007; Young et al., 2007)? 4) Was it thick (Root et al., 2005) or thin (e.g., Ernst and Peacock, 1996)? 5) Did the bulk of the crust transform to high-pressure phases or was the transformation limited to mafic material (e.g., Ernst, 2006)? A successful model must predict the deformational structures and the *P–T–t* path observed for the WGR. The purpose of this study is to address the timing and rates of exhumation, cooling, and melting of the WGR through the geochronology of phases associated with the amphibolite-facies overprint of the WGR.

1.1. Geochronology of sphene and rutile

To be well suited for dating a post-(U)HP amphibolite-facies overprint, a mineral must either i) have an amphibolite-facies closure

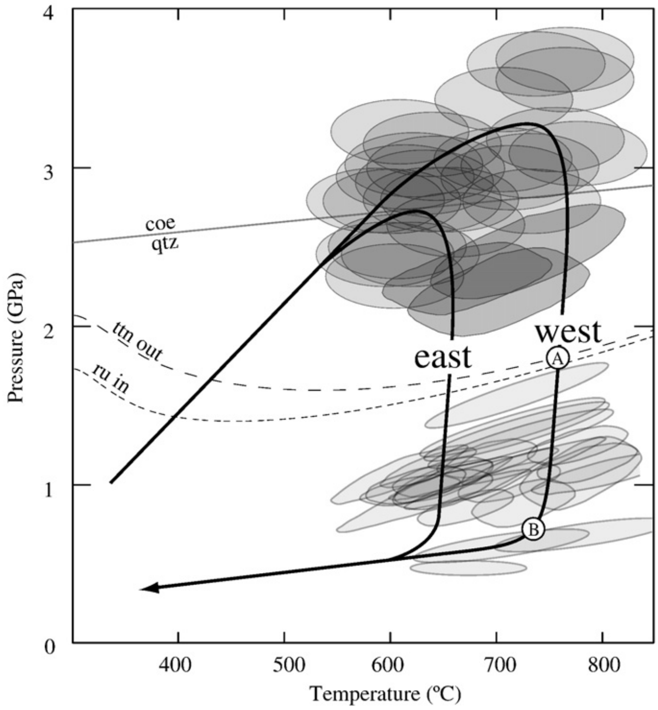

Fig. 2. P–T history of the Western Gneiss Region after Hacker (2006), showing peak conditions of ~750 °C and 3.4 GPa, followed by near-isothermal decompression to mid-crustal levels. Rutile (ru) and titanite (ttn) stability curves are approximated using Perple_X (Connolly, 1990) and a granodioritic composition typical of the WGR. Location of stability curves varies little with moderate changes in composition. Along the western P–T path, titanite could crystallize at anypoint between points A and B.

temperature (T_c), such that it loses all of its radiogenic daughter product during the event, ii) be unstable at UHP depths and grow *de novo* during decompression/retrogression from the breakdown of HP assemblages, or iii) crystallize within post-(U)HP amphibolite-facies melts. U–Pb titanite geochronology is ideal in this regard. The T_c of titanite depends on grain size and cooling rate and has been estimated both experimentally (Cherniak, 1993) and from field observations to be >650 °C (for a review, see Frost et al., 2001). Thus, grains that are large enough or remained cool enough to retain their Pb will yield the time of growth, whereas grains that are small or were sufficiently heated will yield cooling ages (for an example of how size relates to T_c, see Table 1). Titanite is also advantageous because it is unstable at UHP in bulk compositions typical of the WGR (Fig. 2). During subduction, as pressure increases, titanite breaks down to form rutile, and during exhumation, the reverse process occurs. Thus, titanites in the higher-grade portions of the WGR likely grew during exhumation, through either the breakdown of rutile or decompression-related melting, and should not have pre-Caledonian inheritance. If decompression occurred over an extended period of time, i.e., longer than a few Ma, however, individual titanite ages may be somewhat difficult to interpret. Because mineral reactions, and therefore retrogression and decompression melting, are aided by heat, deformation and fluid, titanite may form at any stage during decompression when it is stable and temperatures are still high, i.e. from ~1.8 to 0.6 GPa (Fig. 2).

The U–Pb rutile technique also shows promise, although the U–Pb systematics of rutile are poorly understood. Experimental data suggest a T_c similar to that of titanite (Cherniak, 2000), but field results imply that it could be as much as ~150 °C lower (Mezger et al., 1989). The common presence of ilmenite exsolution lamellae in WGR rutile suggests that the effective diffusion lengthscale in rutile may be much less than the grain size. In contrast to titanite, in bulk compositions typical of the WGR, rutile is stable at high pressure, and unstable at low-pressure amphibolite-facies conditions (Fig. 2). Thus, depending on effective grain size, rutile will either yield crystallization ages representing burial of the WGR, or cooling ages locked in during exhumation. In this study rutile was sampled from rocks that preserve high-pressure assemblages (typically eclogite) and titanite was sampled from the matrix of the common WGR orthogneiss and from leucosomes within the gneiss.

1.2. Previous geochronology

The timing of UHP metamorphism was first estimated by Krogh et al. (1974), and later confirmed by Griffin and Brueckner's (1980) pioneering work using Sm–Nd geochronology on eclogites. They retrieved ages ranging from 447 Ma to 407, and concluded that the average age of ~425 Ma was the best estimate for this event. Subsequent work, employing Lu–Hf, Sm–Nd and U–Pb geochronology, yielded HP ages from ~420 to 398 (Mearns, 1986; Mørk and Mearns, 1986; Terry et al., 2000a; Carswell et al., 2003a,b; Krogh et al., 2004; Root et al., 2004; Kylander-Clark et al., 2007a,b; Young et al., 2007); Kylander-Clark et al. (2007a,b) concluded that the ~20 Ma span represents protracted burial from the initial stages of HP mineral growth to peak conditions.

The timing of amphibolite-facies metamorphism in the WGR has been estimated using two different approaches. Krogh et al. (2004) and Terry et al. (2000a) dated minerals with a T_c higher than the amphibolite-facies peak temperatures: zircon from amphibolite-facies pegmatites gave U–Pb ages of ~395 Ma on Averøya, Fjørtoft and Flemsøya (Krogh et al., 2004), and monazite from the matrix of a microdiamond-bearing gneiss on Fjørtoft yielded U–Pb ages of 397.5 ± 4.4 Ma (Fig. 3, Terry et al., 2000a). Both these ages were interpreted to date amphibolite-facies metamorphism; however, because of the possibility of inheritance, these ages are maxima.

Tucker et al. (1987, 1990, 2004) used U–Pb dating of titanite to discern the timing of the amphibolite-facies overprint. They produced over 50 ages from the northern portion of the WGR (Fig. 3), providing considerable insight into the timing of this event. All their data fall on a single discordia line between 1657 ± 3 Ma and 395 ± 3 Ma, from which Tucker et al. made two key observations. First, northwest of what they termed the 'Sveconorwegian boundary' (Fig. 3), there was only one significant geologic event since ~1650 Ma—the Caledonian orogeny; south of that boundary, there was a significant regional thermal event at ca. 950 Ma (Tucker et al., 2004). Second, the amphibolite-facies event during the Caledonian occurred everywhere at the same time: 395 Ma. The latter observation directly pertains to the rates of exhumation and cooling of the WGR, but has limitations: 1) most of the data are discordant and thus provide limited control on the timing of Pb loss or neocrystallization at any given location, and 2) the areal extent of the data has minimal overlap with the area in which peak metamorphic ages and $^{40}Ar/^{39}Ar$ muscovite cooling ages have been measured.

Cooling through ~400 °C during the post-(U)HP amphibolite-facies overprint (Fig. 2) is recorded by $^{40}Ar/^{39}Ar$ muscovite ages, which decrease from ~400 Ma in the eastern WGR to ~374 Ma in the western WGR (Fig. 3; summary in Hacker, 2007). These ages most likely correspond to mid-crustal depths of 15–20 km, following cooling from 750 °C and 0.6 GPa (Schärer and Labrousse, 2003; Root et al., 2005). They show that the retrograde path from UHP conditions to cooling below 400 °C locally spanned as much as ~25 Ma.

The dataset presented in this paper builds on that of Tucker et al. (1987, 1990, 2004). It has the additional advantages that i) the sampled region has yielded many eclogite-facies and cooling ages, providing a sound basis for broader reconstruction of the P–T–t history; and, ii) a higher percentage of the ages are concordant. Both these factors allow improved determinations of the exhumation and cooling rates over a large area of the WGR.

2. Methods and sample descriptions

Titanite samples were collected i) as matrix minerals within the gneiss and ii) from leucosomes (Table 1). Titanites occur within the

Table 1
Mineralogy modes of titanite and rutile samples from the Western Gneiss Region, Norway

Sample	qz	pl	kfs	mu	bt	amp	cpx	opx	grt	zrn	cc	ep/zo	ap	opq	ttn	rt	Size (μm)	T_c[a]
Titanite samples																		
1. P5630A1	10	20	20		15	10			10	t		r	r	r	r		100–300	605–645
2. P6815E1[b,c]		60	10		5	20						r			r		<300	645
3. Y1710C5[b,c]	10	50			10	20								5	5		10,000	815
4. R9826C1	10	10	40		15	15					r				t		1000	700
5. 8907B6	20	20	40		5	10			r	t		r			r		500	670
6. R9823F8[b,c]	20	55			20										5		10,000	815
7. P5626P1	15	25	20			15			20	t			r		r		500	670
8. P5626M2[b,c]	10	80				10									t		1000	700
9. P5701G[b,c]	25	15	30		20										5		>1000	700
10. P6820E2[b]	20	45			30										r		>1000	700
11. K5702D1[b,c]	20	60			10	10									r		1000	700
12. P5625F2[b,c]	15	15				60						5			5		5000	780
13. E9808D9[b,c]	15	40	10		5	20									5		>1000	700
14. P6818D1[b,c]	20	35	35		5										5		>1000	700
15. E9805P8	40	35			20	r									r		200	630
16. E9805K9	5	40			10	20			20	t		r	r		r		200–500	630–670
17. E9816D7	15	50			15	15				t		r	t		r		500–1000	670–700
18. E9804D5[b,c]	20	70				20						r			r		>1000	700
19. E1616C8[b,c]	20	35			20	20									r		1000	700
20. E9801S[b]	15	50	15		10	5						r			5		1000	700
21. K7710E1[b,c]	20	35	25			10						r			r		>1000	700
22. P6808A2	35	25			15				15	t		5			r		200–500	630–670
23. P6813B1	25	25	15		15							15		t	5		500+	670
Rutile samples																		
1. P6807G1	30	20		20	15				15	t		r				r	100–300	645–705
2. K7718E	90															10	5000	735
3. R9826J					10		50		40	t						r	500	735
4. 8906A11							35	35	25	t						r	<1000	780
5. 8830B	80															20	10,000	970
6. R3703A2					5		30	30	30							r	50–200	610–680

Mineral abbreviations follow Kretz (1983); r = rare (<2 vol%), t = trace (<0.5 vol%).
[a] Closure temperature estimated following Cherniak (1993; 2000).
[b] Hand sample analysis only.
[c] Leucosome.

typical granodioritic to tonalitic WGR gneiss in association with biotite and plagioclase, K-feldspar, quartz and/or hornblende. The titanite is commonly euhedral to subhedral, aligned within the foliation, and ~100 μm to a few mm in size. Leucosomes in the WGR are generally decimeter-scale, equigranular *in situ* melts, consisting of quartz, plagioclase ± alkali feldspar, titanite and either biotite or hornblende. They comprise 2–50 vol.% of typical outcrops. Titanite in leucosomes is typically euhedral and of mm size. Rutile was collected from 6 samples: 3 unretrogressed eclogites, one garnet-bearing gneiss, and 2 cm-scale veins within eclogites from the western portion of the WGR. It is generally xenoblastic, ranging in size from ~100 μm to several mm (Table 1).

Analyzed fractions were hand picked to exclude any inclusions, following disk mill and Frantz isodynamic magnetic separation. Except for a few exceptions in which grain size was small enough (<500 μm), separates were picked from pieces of individual grains rather than whole grains. They were then washed in weak HNO_3, a mixed ^{235}U–^{205}Pb spike was added, and the samples were dissolved in a 10:1 HF–HNO_3 in Parr bombs. Chemical procedures follow that outlined in Mattinson (2005). Solutions were passed through Dowex AG 1x8 resin in 1 N HBr to separate Pb from matrix. Pb separates were then passed through the same resin in 3.1 N HCl for further purification and the matrix was passed through UTEVA resin in 2 N HNO_3 for separation of U. Analysis was performed on the Finnigan MAT-261 at the University of California, Santa Barbara. Common Pb was corrected using a matrix mineral with a low U/Pb ratio, typically using feldspar (gneiss) or clinopyroxene (eclogite) analyzed from the same sample. Analysis of common Pb minerals followed that listed above, except that fractions were first leached in 7 M HNO_3 on a hot plate.

3. Results

Results for titanite (n=23) and rutile (n=6) analyses are listed in Table 2 and shown in Figs. 3 and 4. The relative common Pb contents vary greatly among the samples, with $^{206}Pb/^{204}Pb$ of 26–769 for titanite and 102–8142 for rutile. The magnitude of common Pb correction is generally reflected in the 2σ age errors, which range from 0.2% to 0.7% for the $^{238}U/^{206}Pb$ ages and 0.2% to 4.2% for the $^{235}U/^{207}Pb$ ages.

The concordant titanite ages range from 401 to 390 Ma (n=10) with the bulk of ages between 393 and 390 Ma (n=7). In general, the concordant titanite ages are ~4–5 Ma older than $^{40}Ar/^{39}Ar$ muscovite ages from nearby locations, with the oldest ages in the east and the youngest in the west. Most of the titanite data, however, are limited to a region where the muscovite ages are 390–385 Ma, and two samples (P6820E2 and E9805P8) are more than 5 Ma older than nearby muscovite ages (Fig. 3). The ~401 Ma age from sample E9805P8 should be viewed with caution; although it overlaps concordia, its centroid is discordant and consistent with the discordia array.

In conjunction with the 7 youngest, concordant titanite data, the discordant titanite data lie on (n=9) or between (n=3) two discordia lines: one with a lower intercept of 387±9 Ma and an upper intercept of 938±21 Ma, and a second with lower intercept of 389±3 Ma and an upper intercept of 1635±9 Ma. The '389–1635 Ma' discordia line is similar to that produced by Tucker et al. (1987, 1990, 2004); all data (this study *and* Tucker et al.) northeast of Tucker et al.'s Sveconorwegian boundary (Fig. 3) lie on that discordia line. Southwest of this boundary, data fall on or between the two discordia lines. In general, the ages from the hot core of the orogen (the western and northern portions of the study area) are closer to the lower intercept—a trend that, with a few

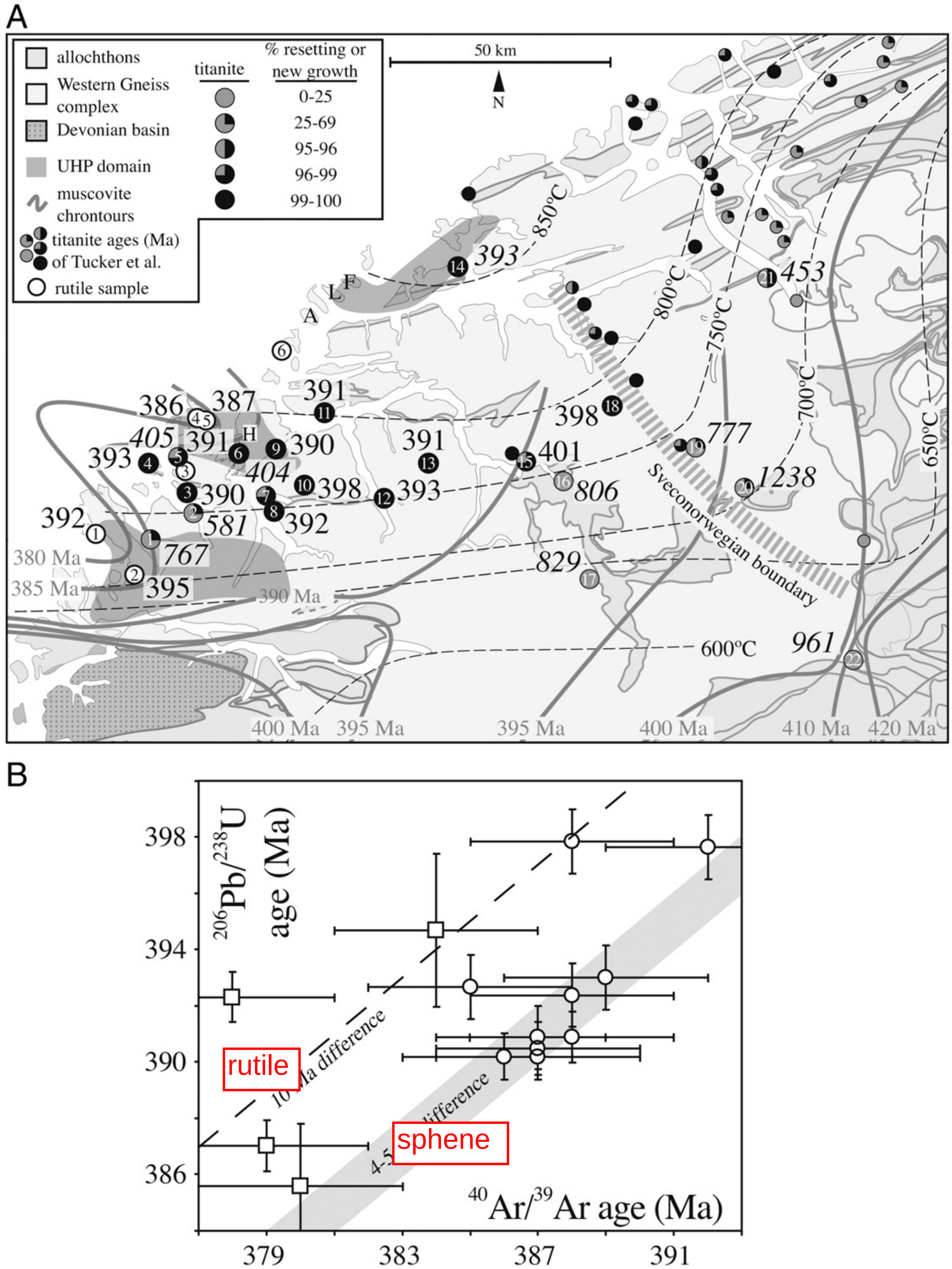

Fig. 3. A) U–Pb titante and rutile data from the Western Gneiss Region produced in this study and by Tucker et al. (1987, 1990, 2004). $^{238}U/^{206}Pb$ ages are reported in Ma; discordant data are in italics. Amphibolite-facies zircon and monazite ages (see text): A = Averøya, L = Lepsøya, F = Fjortoft, H = Hareidlandet, N = Leinøya, V = Volda. Muscovite data (Hacker et al., 2006) is contoured by age. B) Concordant data plotted against approximate $^{40}Ar/^{39}Ar$ muscovite age. Squares show rutile ages; the two southernmost ages (rutile locations 1 and 2) are >10 Myr older than mu ages, whereas the two northern ages (locations 4 and 5) are 5–10 Ma older. Rutile ages that are thought to be discordant (locations 3 and 5; see text) are not shown for clarity. Titanite ages (circles) are ~4–5 Ma older than nearby muscovite ages.

exceptions, mirrors the increase in peak temperature (Krogh, 1982). Away from the core of the orogen, in the direction of the foreland, the apparent ages show a marked increase over a short distance. For titanite, this jump—~400 Ma in $^{238}U/^{206}Pb$ ages—is ~50–70 km inland, and occurs over a few km. A similar trend is seen in titanite data farther north (Tucker et al., 1987, 1990, 2004), but there the strongly inherited grains are closer to the coast. There is no apparent age trend based on whether or not the titanite was sampled from a leucosome or from within the gneiss; both groups span a similar age range over the same area. The easternmost and southernmost sample locations, P6808A2 and P6813B1, yield the two least reset ages. Temperature estimates from near these localities range from ca. 580 °C to 650 °C (Cuthbert et al., 2000; Hacker et al., 2003; Walsh and Hacker, 2004).

Three of the 6 rutile ages are concordant and range from 392 to 385 Ma. The oldest discordant age (K7718E) is from a quartz+rutile vein in eclogite, and could therefore have been out of equilibrium with the omphacite used for the common Pb correction. It is possible that vein rutile contains an inherited component, such as zircon, however, small

Table 2
U–Pb data for titanite and rutile from the Western Gneiss Region, Norway

Sample	Mass	U	Common Pb[1]		$^{206}Pb^2$	$^{208}Pb^2$	$^{207}Pb^3$	Error	$^{206}Pb^3$	Error	corr. coeff.	Ages (Ma)	
			$^{206}Pb^2$	$^{207}Pb^2$	^{204}Pb	^{206}Pb	^{235}U	(%)	^{238}U	(%)		^{206}Pb	^{207}Pb
	(mg)	(ppm)	^{204}Pb	^{204}Pb								^{238}U	^{235}U
Titanite analyses													
1. P5630A1 (lyb)	1.7	31	17.05	15.45	59	1.214	1.186	0.86	0.12639	0.43	0.507	767.2 (3.3)	793.9 (6.8)
2. P6815E1 (lyb)	1.3	11	18.04	15.57	37	1.319	0.814	2.1	0.09426	0.70	0.326	580.7 (4.1)	604.5 (13)
3. Y1710C5 (lb)	NA	NA	17.82	15.55	141	0.341	0.4693	0.53	0.06239	0.29	0.538	390.2 (0.8)	390.7 (1.5)
4. R9826C1 (b)	3.0	50	17.50	15.54	145	0.338	0.4701	0.42	0.06281	0.29	0.682	392.7 (1.1)	391.3 (1.6)
5. 8907B6 (lyb)	1.3	45	17.32	15.48	89	0.500	0.5044	0.69	0.06482	0.23	0.333	404.9 (0.9)	414.7 (2.9)
6. R9823F8 (lyb)	3.2	28	17.20	15.45	36	1.607	0.480	2.1	0.06244	0.24	0.114	390.5 (0.9)	398.4 (8.4)
7. P5626P1 (y)	2.2	12	17.17	15.46	26	1.510	0.513	4.2	0.06472	0.29	0.069	404.3 (1.2)	420.5 (18)
8. P5626M2 (ly)	NA	NA	18.27	15.46	182	0.250	0.4759	0.37	0.06276	0.29	0.771	392.4 (1.1)	395.2 (1.5)
9. P5701G (db)	NA	NA	17.41	15.51	365	0.321	0.4700	0.34	0.06240	0.30	0.874	390.2 (0.8)	391.2 (0.9)
10. P6820E2 (db)	1.3	241	18.50	15.62	271	0.318	0.4793	0.33	0.06366	0.29	0.879	397.8 (1.1)	397.6 (1.3)
11. K5702D1 (yb)	2.1	68	17.77	15.53	71	0.553	0.4698	0.80	0.06251	0.29	0.361	390.9 (1.1)	391.0 (3.1)
12. P5625F2 (lb)	1.0	12	18.08	15.58	103	0.476	0.4730	0.55	0.06286	0.29	0.526	393.0 (1.1)	393.2 (2.1)
13. E9808D9 (b)	0.6	87	17.54	15.50	310	0.334	0.4707	0.33	0.06251	0.23	0.713	390.9 (0.9)	391.7 (1.3)
14. P6818D1 (yb)	0.7	74	17.64	15.50	155	0.287	0.4757	0.46	0.06278	0.29	0.629	392.5 (1.1)	395.1 (1.8)
15. E9805P8 (lb)	0.5	35	17.26	15.43	101	0.543	0.4881	0.73	0.06421	0.24	0.328	401.2 (1.0)	403.6 (3.0)
16. E9805K9 (y)	0.9	19	17.03	15.47	70	0.869	1.2556	0.65	0.13324	0.29	0.440	806.3 (2.3)	825.9 (5.4)
17. E9816D7 (db)	0.8	104	17.82	15.56	384	0.817	1.3234	0.35	0.13737	0.34	0.971	829.8 (2.8)	856.0 (3.0)
18. E9804D5 (db)	0.7	123	16.95	15.45	638	0.164	0.4796	0.29	0.06363	0.29	0.977	397.6 (1.1)	397.8 (1.2)
19. E1616C8 (db)	1.4	135	18.52	15.62	237	1.153	1.4399	0.28	0.12809	0.23	0.795	777.0 (1.8)	905.7 (2.6)
20. E9801S (db)	1.8	188	17.17	15.48	769	1.099	2.8018	0.29	0.21169	0.29	0.995	1237.8 (3.6)	1356.0 (3.9)
21. K7710E1 (b)	0.5	332	17.91	15.49	320	0.545	0.6276	0.26	0.07281	0.23	0.860	453.1 (1.0)	494.6 (1.3)
22. P6808A2 (db)	0.7	25	18.37	15.58	69	0.564	1.600	0.89	0.16083	0.24	0.264	961.4 (2.3)	970.3 (8.7)
23. P6813B1 (db)	1.7	197	17.61	15.54	446	0.518	1.5035	0.33	0.15152	0.32	0.978	909.5 (2.9)	931.8 (3.1)
Rutile analyses													
1. P6807G1 (rb)	0.8	17	18.56	15.60	102	0.389	0.4774	1.0	0.06275	0.23	0.227	392.3 (0.9)	396.3 (4.3)
2. K7718E (dbr)	0.6	20	17.91	15.48	414	0.093	0.4817	0.70	0.06314	0.69	0.987	394.7 (2.7)	399.2 (2.8)
3. R9826J (r)	0.8	170	18.64	15.59	581	0.066	0.4588	0.30	0.06103	0.29	0.971	381.9 (1.1)	383.4 (1.1)
4. 8906A11 (dbr)	2.1	117	17.48	15.53	575	0.067	0.4638	0.30	0.06172	0.29	0.970	386.1 (2.2)	386.9 (2.3)
5. 8830B (r)	6.9	5	18.69	15.59	8142	0.005	0.4650	0.24	0.06188	0.24	0.877	387.0 (0.9)	387.7 (0.9)
6. R3703A2 (r)	1.6	36	18.41	15.53	477	0.083	0.4583	0.37	0.06090	0.36	0.973	381.1 (1.4)	383.1 (1.4)

[1]Common Pb was analyzed on low U/Pb feldspar (to correct titanite) or clinopyroxene (to correct for rutile). No significant U concentration was detected in common Pb fractions.
[2]Measured ratio corrected for fractionation only.
[3]Corrected for fractionation, spike, and initial common Pb. Blank was considered negligible.
Colors of grains are listed in parentheses: d = dark, l = light, b = brown, y = yellow, r = red.
Analysis accomplished with a Finnigan MAT-261 thermal ionization mass spectrometer at the University of California Santa Barbara. Decay constants used are $^{238}U = 0.155125 \times 10^{-9}$ yr^{-1}, and $^{235}U = 0.98485 \times 10^{-9}$ yr^{-1} (Steiger and Jäger, 1977).

changes in the common $^{207}Pb/^{204}Pb$ ratio would yield concordance, and thus we prefer the $^{238}U/^{206}Pb$ age of 395 Ma. The two younger discordant points (R3703A2 and R9826J) may have suffered minor recent Pb loss, in which case their $^{207}Pb/^{206}Pb$ ages of ~395–393 Ma may be more representative of the age of metamorphism. These two data are thus ignored henceforth.

Rutile ages generally young northward. In the Nordfjord UHP domain, the $^{238}U/^{206}Pb$ ages are 395±3 Ma and 392±1 Ma, more than 10 Ma older than nearby $^{40}Ar/^{39}Ar$ muscovite ages; in the Sørøyane UHP domain, the $^{238}U/^{206}Pb$ ages of 386±1 and 387±1 Ma are 5–10 Ma older than nearby $^{40}Ar/^{39}Ar$ muscovite ages (Fig. 3).

4. Discussion

What, precisely, are the geologic implications of these ages? Although, the T_c for titanite is commonly cited to be 650 °C or greater, and we found two titanite samples (P5630A1 and P6815E1) from regions that experienced temperatures in excess of 700 °C that show strong preservation of an inherited component. Both are composed of grains smaller (<500 μm) than most samples analyzed in this study, which would imply that most samples from this study did not exceed the T_c for titanite and thus likely crystallized during the Caledonian event. Further evidence for this comes from a concordant $^{238}U/^{206}Pb$ age of 398±1 Ma (P6820E) that is older than several ages to the east; this sample experienced higher temperatures and cooled later than the younger titanites collected from colder rocks farther east (e.g., P5626F2). This sample is from a leucosome, and likely dates the timing of melting and recrystallization during early stages of exhumation, rather than cooling, which followed the bulk of the exhumation. Some titanites could have undergone diffusion during exhumation and initial cooling, in the presence of deformation, fluids or both; in fact Tucker et al. (2004) concluded, based on consistently reproducible, discordant data, that the 395 Ma event represented in their dataset was caused by both Pb loss and new titanite growth. We conclude that our dataset, which spans several Ma within limited areas and contains both small and large titanite that experienced a range in peak temperatures, records the duration of the decompression event. The oldest concordant ages indicate a maximum depth of ~1.8 GPa, and the youngest concordant and lower intercept ages indicate a minimum depth of 0.6 GPa. This dataset thus allows us to distinguish two separate events during the post-peak *P–T–t* path of the WGR: 1) exhumation from peak depths of up to 120 km to mid-crustal levels, and 2) cooling from 600–800 °C to 400 °C (see below).

The rutile ages from this study are younger than the ages of WGR peak metamorphism. The fact that we observe a similar age difference between titanite and nearby $^{40}Ar/^{39}Ar$ muscovite ages *and* between rutile and nearby $^{40}Ar/^{39}Ar$ muscovite ages in the Sørøyane UHP domain suggests that the T_c of rutile is similar to that of titanite in that

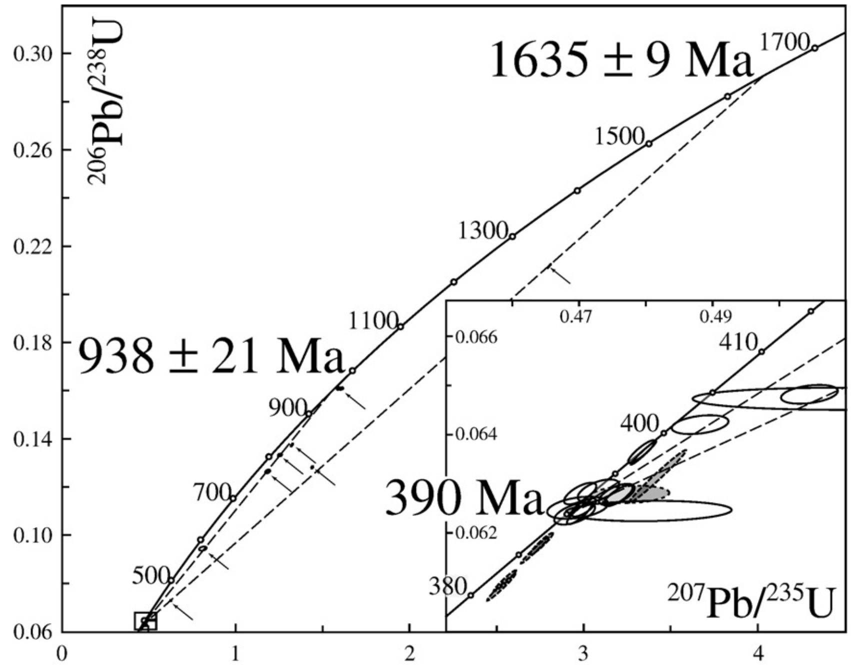

Fig. 4. Concordia plot, showing all titanite (solid outline) and rutile data (dashed outline). Small, discordant points are highlighted with an arrow.

domain. A true comparison is difficult, however, because the sample locations are several km apart and have equivalent $^{40}Ar/^{39}Ar$ muscovite ages that differ by 5 Ma; different spatial and/or temporal cooling rates could have produced a variety of cooling ages in minerals with the same or different closure temperatures. In fact, rutile ages in the Nordfjord UHP domain may be ~5–10 Ma older than those in the Sørøyane UHP domain (Fig. 3) because of lower peak temperatures (650–750 °C vs. >750 °C) and hence slower Pb diffusion, or because of more rapid initial cooling followed by slower cooling. This possible difference in cooling history might have been controlled by proximity to the unroofing structure (e.g., the Nordfjord–Sogn Detachment, which is thought to be responsible for the majority of exhumation, Andersen et al., 1994; Engvik and Andersen, 2000; Johnston et al., 2007).

Coupled with their *P–T*-dependent growth history, the unique, intermediate closure temperatures of titanite and rutile allow better estimates of the exhumation and cooling rates, which in turn aid in understanding the processes involved in the evolution of the Western Gneiss UHP terrane. Furthermore, the Pb diffusivity and *P–T*-dependent stability of titanite and the regional distribution of discordant ages allow us to make interpretations about titanite transformation during the burial and exhumation of continental crust.

4.1. Exhumation of the WGR

As stated above, titanites are likely to have crystallized between ~1.8 and 0.6 GPa, during decompression, after titanite had become stable, but before the WGR began to cool. The youngest titanite will yield the point at which the WGR passed through ~0.6 GPa and the oldest concordant age should pinpoint passage through ~1.8 GPa. A leucosome in the Sørøyane UHP domain yielded concordant titanite with the youngest $^{238}U/^{206}Pb$ age: 390.2±0.8 Ma (P5701G; Fig. 3). The more precise of the two lower intercepts from each discordia array, 389±3 Ma, supports the conclusion that this age likely corresponds to the time of initial cooling at ~0.6 GPa. The best estimate for the age of UHP conditions nearby is the 401.6±1.6 Ma (795 °C and 3.2 GPa; Carswell et al., 2003b) Hareidlandet eclogite, ~10 km to the WNW (Fig. 3). Assuming a density of 3 g/cm^3, the crust in this area was thus exhumed from ~105 km to ~20 km in ~12 Ma, an exhumation rate of ~7 mm/yr. These rates are slower than estimates from other, smaller UHP terranes such as the Dora Maira (Rubatto and Hermann, 2001) and Kaghan Valley terranes (Parrish et al., 2006), but similar to other large UHP terranes, such as the Dabie–Sulu terrane of eastern China (>2 mm/yr, Hacker et al., 2000). This suggests that there may be a fundamental difference in the mechanisms controlling the evolution of large UHP terranes, like the Dabie–Sulu and WGR, which undergo protracted subduction (Hacker et al., 2006; Kylander-Clark et al., 2007b) and exhumation (this study, Hacker et al., 2000) and smaller ones, which undergo rapid subduction and exhumation (e.g., Rubatto and Hermann, 2001; Leech et al., 2005; Parrish et al., 2006).

4.2. Cooling of the WGR

The fact that the WGR rose relatively slowly from mantle depths of >100 km to mid-crustal depths of ~20 km and yet remained nearly isothermal requires that it was thermally isolated by an ~15 km-thick thermal 'blanket' (Root et al., 2005). The subsequent rate of cooling at crustal depths can reveal whether this blanket remained intact and erosion was the principal unroofing mechanism through crustal depths or whether the effective thermal diffusion distance must have been reduced through tectonic unroofing.

Because the peak metamorphic ages, $^{40}Ar/^{39}Ar$ muscovite ages, and U–Pb titanite and rutile ages vary spatially, and because the T_c of titanite and rutile depend on grain size, establishing cooling rates requires careful consideration. The more precise lower intercept of the two discordia arrays formed by the titanite data implies that a thermal event occurred at 389±3 Ma. Most of the titanite samples recording this thermal event are from locations where the $^{40}Ar/^{39}Ar$ muscovite ages range from 390 to 385 Ma. This observation, combined with the observation that *concordant* titanite and rutile analyses are no less than 4 Ma older than nearby $^{40}Ar/^{39}Ar$ muscovite ages, implies that temperatures dropped from near-peak temperatures of ~750 °C to ~400 °C in ~4 Ma, a cooling rate of ~90 °C/Ma. Conductive cooling of 750 °C to 400 °C of a crustal unit at 15–20 km depth requires a significantly longer period of 12 Ma (assuming a semi-infinite

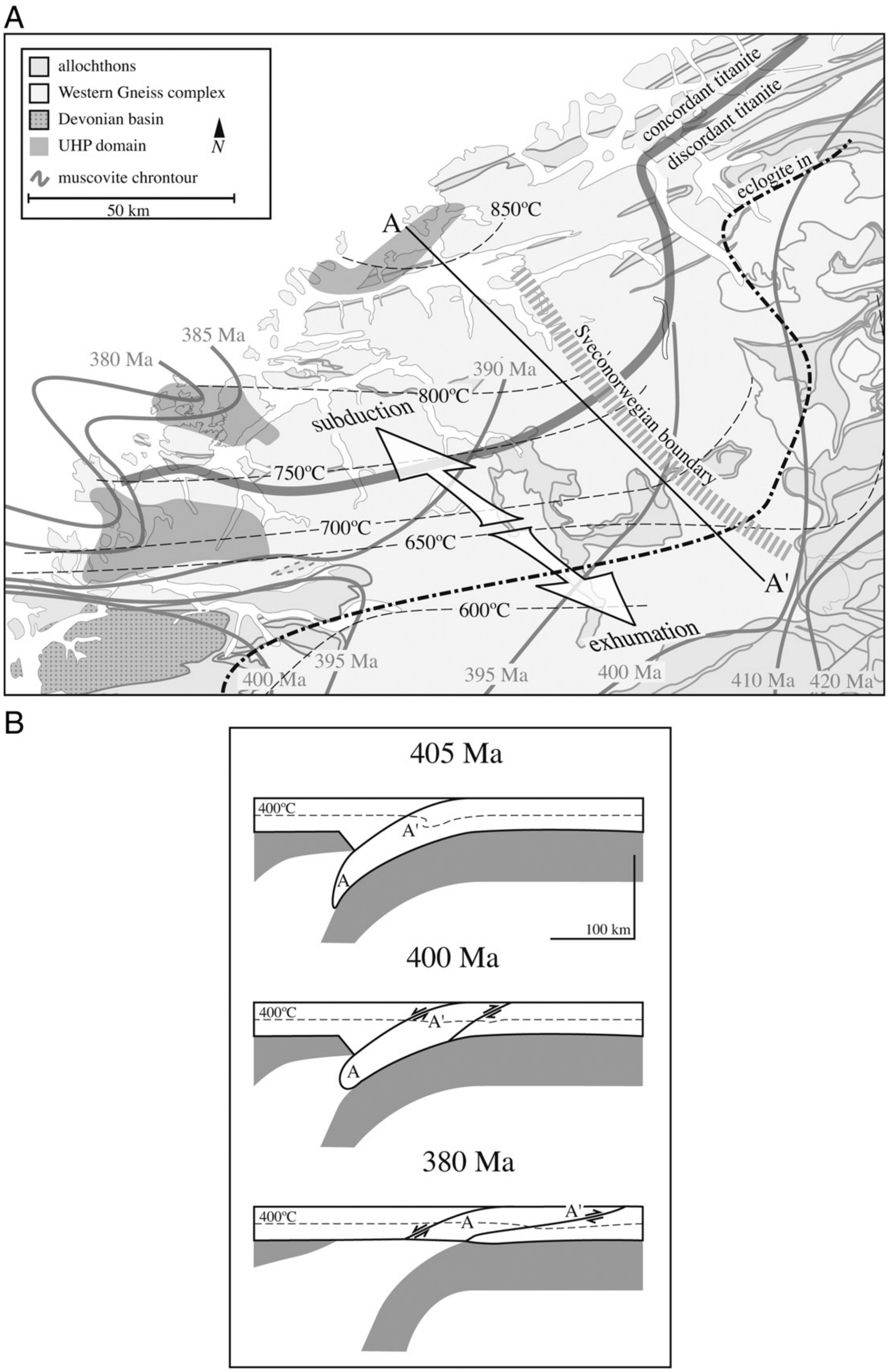

Fig. 5. A) Western Gneiss Region, showing approximate boundary between concordant and discordant titanite data and titanites affected by the Sveconorwegian event (Tucker et al., 1990; Tucker et al., 2004; this study), and the eclogite in boundary. B) Cross section A–A′ at near-peak conditions (405 and 400 Ma) and following cooling through 400 °C of the UHP regions (380 Ma).

half-space, a thermal diffusivity = 1 mm^2/s and a surface temperature of 0 °C). The shorter time of ~4 Ma given by dating implies that the cooling was effected by tectonic unroofing, such as the extension along the Nordfjord–Sogn Detachment (e.g., Andersen et al., 1994; Johnston et al., 2007), thrust of the WGR over the foreland, or a combination of the two.

4.3. Exhumation style and crustal transformation

In this section we examine the predictions of the tectonic models presented in the introduction, focusing on the data presented in this paper.

1) Was the WGR exhumed as one coherent body, a few large bodies, or was it well mixed/disrupted? The westward-younging gradient in titanite and rutile ages mimics that of the $^{40}Ar/^{39}Ar$ muscovite ages, and implies that the central WGR was progressively unroofed as a coherent slab from east to west, beginning at lower to mid-crustal depths (titanite/rutile) and continuing through mid-crustal levels (muscovite). The WNW-increasing *P–T* gradient, the well-defined boundary between concordant and discordant titanite ages, and the similarity between muscovite cooling ages in the east and eclogite ages in the west suggest that the WGR remained coherent throughout its entire exhumation history, with UHP domains at near-peak conditions while the shallower eastern end of the slab, nearly 100 km up dip, was beginning to cool through 400 °C (Fig. 5). The sharp boundary between concordant and discordant titanite data parallels the 'eclogite-in' boundary (Fig. 5), supporting the inference that the slab was coherent from eclogite facies through exhumation. The northward bend, apparent in both boundaries, implies a northeastward decrease in depth of exhumation.
2) Did the WGR stall and flatten at the Moho or was it progressively exhumed at constant rates? Because titanite at the eastern end of the WGR exhibits significant inheritance, the data presented in this paper shed little light on this model. However, because UHP eclogites in the western WGR have ages identical to muscovites in the eastern WGR, the shallow, eastern portions of the slab must have been exhuming through the crust while the UHP eclogites were still at depth.
3) Did the slab rise as a diapir through the mantle or was it extruded as a slab? As suggested above, the WGR was a relatively coherent body during exhumation, with little mixing, which favors the slab-exhumation model. Furthermore, if the slab rose through the hot mantle, rather than back up the chilled subduction zone, its shallow portion would have heated more, producing melts and Pb loss in titanite. All the eastern titanite samples, which include 2 leucosomes, yield old ages, implying that little melting and Pb loss occurred in this region during the Caledonian event.
4) Was the exhumed slab thick or thin? As presented above, exhumation from 100 km to 20 km may have taken as long as ~12 Ma. A one-dimensional thermal model (Root et al., 2005) yielded a minimum thickness of 30 km for the exhumed slab.
5) Did the bulk of the WGR crust transform to eclogite facies or did only the mafic material transform? As stated above, the concordant ages obtained in this study are likely the result of neocrystallization during the Caledonian event, rather than Pb loss. This implies that the slab down dip (WNW) of the concordant–discordant boundary had transformed to a HP mineral assemblage that included a HP Ti-bearing phase other than titanite, i.e. rutile, which subsequently broke down to form titanite during decompression. This boundary is also approximately equivalent to the 750 °C peak T isotherm (Fig. 5), suggesting that i) titanite was unstable above this temperature or ii) mineral reactions were too sluggish below this temperature to permit recrystallization in the relatively dry gneisses. Because the stability of titanite depends primarily on pressure (Fig. 2), the first possibility only can be correct if peak isobars are parallel to the 750 °C peak isotherm. Peak pressures are more difficult to obtain than peak temperatures; however, because coesite is found in the west and not in the east at temperatures below 750 °C (Fig. 3), the latter possibility appears more likely.

5. Conclusions

Data presented in this paper provide insight into the style and rates at which the WGR UHP terrane was exhumed from mantle depths. We conclude that the WGR was progressively exhumed, at rates of ~7 mm/yr, as a thick, coherent slab, likely reversing its WNW-dipping subduction route. Exhumation through crustal levels was effected by tectonic unroofing, and began first in the eastern and southern WGR while the northwest portion was still at or near UHP depths. The hotter, higher-pressure portion of the crust retrogressed from its high-pressure assemblages during decompression, and local *in situ* melting occurred. Exhumation of the UHP domains to mid-crustal levels was complete by ~390 Ma and rapid cooling of ~90 °C/Ma ensued via tectonic unroofing, almost 10 Ma after the shallowest eclogites had cooled through 400 °C.

Acknowledgements

Substantially improved by thoughtful reviews from F. Corfu, R. Carlson, and an anonymous reviewer. Discussions in the field provided by T. B. Andersen and E. Peterman were most helpful. Funded by NSF EAR-0510453 and EAR-0549674.

References

Andersen, T.B., 1998. Extensional tectonics in the Caledonides of southern Norway, an overview. Tectonophysics 285, 333–351.
Andersen, T.B., Osmundsen, P.T., Jolivet, L., 1994. Deep crustal fabrics and a model for the extensional collapse of the southwest Norwegian Caledonides. J. Struct. Geol. 16, 1191–1203.
Carswell, D.A., Brueckner, H.K., Cuthbert, S.J., Mehta, K., O'Brien, P.J., 2003a. The timing of stabilisation and the exhumation rate for ultra-high pressure rocks in the Western Gneiss Region of Norway. J. Metamorph. Geol. 21, 601–612.
Carswell, D.A., Tucker, R.D., O'Brien, P.J., Krogh, T.E., 2003b. Coesite micro-inclusions and the U/Pb age of zircons from the Hareidland eclogite in the Western Gneiss Region of Norway. Lithos 67, 181–190.
Carswell, D.A., van Roermund, H.L.M., Wiggers de Vries, D.F., 2006. Scandian ultrahigh-pressure metamorphism of Proterozoic basement rocks on Fjortoft and Otroy, Western Gneiss region, Norway. Int. Geol. Rev. 48, 957–977.
Cherniak, D.J., 1993. Lead diffusion in titanite and preliminary results on the effects of radiation damage on Pb transport. Chem. Geol. 110, 177–194.
Cherniak, D.J., 2000. Pb diffusion in rutile. Contrib. Mineral. Petrol. 139, 198–207.
Cuthbert, S.J., Carswell, D.A., Krogh-Ravna, E.J., Wain, A., 2000. Eclogites and eclogites in the Western Gneiss Region, Norwegian Caledonides. Lithos 52, 165–195.
Dobrzhinetskaya, L.F., et al., 1995. Microdiamond in high-grade metamorphic rocks of the Western Gneiss region, Norway. Geology 23, 597–600.
Engvik, A.K., Andersen, T.B., 2000. Evolution of Caledonian deformation fabrics under eclogite and amphibolite facies at Vårdalsneset, Western Gneiss Region, Norway. J. Metamorph. Geol. 18, 241–257.
Ernst, W.G., 2006. Preservation/exhumation of ultrahigh-pressure subduction complexes. Lithos 92, 321–335.
Ernst, W.G., Peacock, S.M., 1996. A thermotectonic model for preservation of ultrahigh-pressure phases in metamorphosed continental crust. In: Bebout, G.E., Scholl, D.W., Kirby, S.H., Platt, J.P. (Eds.), Subduction Top to Bottom. American Geophysical Union, Washington, D.C., pp. 171–178.
Frost, B.R., Chamberlain, K.R., Schumacher, J.C., 2001. Sphene (titanite); phase relations and role as a geochronometer. Chem. Geol. 172, 131–148.
Griffin, W.L., Brueckner, H.K., 1980. Caledonian Sm–Nd ages and a crustal origin for Norwegian eclogites. Nature 285, 319–321.
Griffin, W.L., et al., 1985. High-pressure metamorphism in the Scandinavian Caledonides. In: Gee, D.G., Sturt, B.A. (Eds.), The Caledonide Orogen; Scandinavia and Related Areas. John Wiley & Sons, Chichester, pp. 783–801.
Hacker, B.R., 2006. Pressures and temperatures of ultrahigh-pressure metamorphism: implications for UHP tectonics and H_2O in subducting slabs. Int. Geol. Rev. 48.
Hacker, B.R., 2007. Ascent of the ultrahigh-pressure Western Gneiss region, Norway. Spec. Pap. – Geol. Soc. Am. 419, 171–184.
Hacker, B.R., Gans, P.B., 2005. Continental collisions and the creation of ultrahigh-pressure terranes; petrology and thermochronology of nappes in the central Scandinavian Caledonides. Geol. Soc. Amer. Bull. 117, 117–134.
Hacker, B.R., et al., 2003. Exhumation of high-pressure rocks beneath the Solund Basin, Western Gneiss Region of Norway. J. Metamorph. Geol. 21, 612–629.
Hacker, B.R., et al., 2000. Exhumation of ultrahigh-pressure continental crust in east-central China: Late Triassic–Early Jurassic tectonic unroofing. J. Geophys. Res. 105, 13339–13364.
Hacker, B.R., Wallis, S., Ratschbacher, L., Grove, M., Gehrels, G., 2006. High-temperature geochronology constraints on the tectonic history and architecture of the ultrahigh-pressure Dabie–Sulu Orogen. Tectonics 25, TC5006. doi:10.1029/2005TC001937.
Johnston, S., Hacker, B.R., Ducea, M.N., 2007. Exhumation of ultrahigh-pressure rocks beneath the Hornelen segment of the Nordfjord–Sogn detachment zone, western Norway. Geol. Soc. Amer. Bull. 119, 1232–1248.
Kretz, R., 1983. Symbols for rock-forming minerals. Am. Mineral. 68, 277–279.
Krogh, E.J., 1982. Metamorphic evolution of Norwegian country-rock eclogites, as deduced from mineral inclusions and compositional zoning in garnets. Lithos 15, 305–321.
Krogh, E.J., Mysen, B.O., Davis, G.L., 1974. A Paleozoic age for the primary minerals of a Norwegian eclogite. Ann. Rep. Geophys. Lab. Carnegie Inst. Wash. 73, 575–576.

Krogh, T., Kwok, Y., Robinson, P., Terry, M.P., 2004. U–Pb constraints on the subduction–extension interval in the Averøya-Nordøyane area, Western Gneiss Region, Norway. Goldschmidt Conference Abstract.
Kylander-Clark, A., et al., 2007a. Large-scale, long-lived subduction of ultrahigh-pressure terranes: Western Gneiss Region, Norway. Eos Trans. AGU, 88 (52), Fall Meet. Suppl., Abstract TC22C-02.
Kylander-Clark, A.R.C., et al., 2007b. Coupled Lu–Hf and Sm–Nd geochronology constrains progade and exhumation histories of high- and ultrahigh-pressure eclogites from western Norway. Chem. Geol. 242, 137–154.
Labrousse, L., Jolivet, L., Agard, P., Hébert, R., Andersen, T.B., 2002. Crustal-scale boudinage and migmatization of gneiss during their exhumation in the UHP Province of Western Norway. Terra Nova 14, 263–270.
Labrousse, L., et al., 2004. Pressure–temperature–time–deformation history of the exhumation of ultra-high pressure rocks in the Western Gneiss region, Norway. Spec. Pap. - Geol. Soc. Am. 380, 155–185.
Leech, M.L., Singh, S., Jain, A.K., Klemperer, S.L., Manickavasagam, R.M., 2005. The onset of India–Asia continental collision; early, steep subduction required by the timing of UHP metamorphism in the western Himalaya. Earth Planet. Sci. Lett. 234, 83–97.
Lundmark, A.M., Corfu, F., 2007. Age and origin of the Ardal dike complex, SW Norway: false isochrons, incomplete mixing, and the origin of Caledonian granites in basement nappes. Tectonics 26, TC2007. doi:10.1029/2005TC001844.
Mattinson, J.M., 2005. Zircon U/Pb chemical abrasion (CA-TIMS) method; combined annealing and multi-step partial dissolution analysis for improved precision and accuracy of zircon ages. Chem. Geol. 220, 47–66.
Mearns, E.W., 1986. Sm–Nd ages for Norwegian garnet peridotite. Lithos 19, 269–278.
Mezger, K., Hanson, G.N., Bohlen, S.R., 1989. High-precision U–Pb ages of metamorphic rutile: application to the cooling history of high-grade terranes. Earth Planet. Sci. Lett. 96, 106–118.
Mørk, M.B.E., Mearns, E.W., 1986. Sm–Nd isotopic systematics of a gabbro–eclogite transition. Lithos 19, 255–267.
Parrish, R.R., Gough, S.J., Searle, M.P., Waters, D.J., 2006. Plate velocity exhumation of ultrahigh-pressure eclogites in the Pakistan Himalaya. Geology (Boulder) 34, 989–992.
Roberts, D., Gee, D.G., 1985. An introduction to the structure of the Scandinavian Caledonides. In: Gee, D.G., Sturt, B.A. (Eds.), The Caledonide Orogen–Scandinavia and Related Areas. John Wiley and Sons, Chichester, pp. 55–68.
Root, D.B., et al., 2005. Discrete ultrahigh-pressure domains in the Western Gneiss region, Norway; implications for formation and exhumation. J. Metamorph. Geol. 23, 45–61.
Root, D.B., Hacker, B.R., Mattinson, J.M., Wooden, J.L., 2004. Young age and rapid exhumation of Norwegian ultrahigh-pressure rocks: an ion microprobe and chemical abrasion study. Earth Planet. Sci. Lett. 228, 325–341.
Rubatto, D., Hermann, J., 2001. Exhumation as fast as subduction? Geology 29, 3–6.
Schärer, U., Labrousse, L., 2003. Dating the exhumation of UHP rocks and associated crustal melting in the Norwegian Caledonides. Contrib. Mineral. Petrol. 10.1007, s00410-002-0428-8.
Steiger, R.H., Jäger, E., 1977. Subcommission on geochronology: Convention on the use of decay constants in geo- and cosmochronology. Earth Planet. Sci. Lett. 36, 359–362.
Terry, M.P., Robinson, P., Hamilton, M.A., Jercinovic, M.J., 2000a. Monazite geochronology of UHP and HP metamorphism, deformation, and exhumation, Nordøyane, Western Gneiss Region, Norway. Am. Mineral. 85, 1651–1664.
Terry, M.P., Robinson, P., Ravna, E.J.K., 2000b. Kyanite eclogite thermobarometry and evidence for thrusting of UHP over HP metamorphic rocks, Nordøyane, Western Gneiss Region, Norway. Am. Mineral. 85, 1637–1650.
Tucker, R.D., Krogh, T.E., Råheim, A., 1990. Proterozoic evolution and age-province boundaries in the central part of the Western Gneiss region, Norway: results of U–Pb dating of accessory minerals from Trondheimsfjord to Geiranger. In: Gower, C.F., Rivers, T., Ryan, B. (Eds.), Mid-Proterozoic Laurentia-Baltica. GAC special paper. Geological Association of Canada, St. John's (Newfoundland), pp. 149–173.
Tucker, R.D., Råheim, A., Krogh, T.E., Corfu, F., 1987. Uranium–lead zircon and titanite ages from the northern portion of the Western Gneiss Region, south-central Norway. Earth Planet. Sci. Lett. 81, 203–211.
Tucker, R.D., et al., 2004. Thrusting and extension in the Scandian hinterland, Norway: new U–Pb ages and tectonostratigraphic evidence. Am. J. Sci. 304, 477–532.
van Roermund, H.L., Drury, M.R., 1998. Ultra-high pressure (P> 6 GPa) garnet peridotites in western Norway: exhumation of mantle rocks from > 185 km depth. Terra Nova 10, 295–301.
van Roermund, H.L.M., Drury, M.R., Barnhoorn, A., de Ronde, A., Anonymous, 2001. Relict majoritic garnet microstructures from ultra-deep orogenic peridotites in western Norway. J. Petrol. 42, 117–130.
Wain, A., 1997. New evidence for coesite in eclogite and gneisses; defining an ultrahigh-pressure province in the Western Gneiss region of Norway. Geology 25, 927–930.
Wain, A., Waters, D., Jephcoat, A., Olijnyk, H., 2000. The high-pressure to ultrahigh-pressure transition in the Western Gneiss Region, Norway. Eur. J. Mineral. 12, 667–687.
Walsh, E.O., Hacker, B.R., 2004. The fate of subducted continental margins: two-stage exhumation of the high-pressure to ultrahigh-pressure Western Gneiss complex, Norway. J. Metamorph. Geol. 22, 671–689.
Young, D.J., et al., 2007. Amphibolite to ultrahigh-pressure transition in western Norway: implications for exhumation tectonics. Tectonics 26, TC1007. doi:10.1029/2004TC001781.